Polymer Chemistry

Accepted Manuscript

ROYAL SOCIETY OF CHEMISTRY

www.rsc.org/polymers

Cite this: DOI: 10.1039/c0xx00000x

www.rsc.org/xxxxxx

ARTICLE TYPE

Fibril-shaped aggregates of doxorubicin with poly-L-lysine and its derivative

Lijun Zhu,[a,b] Saina Yang,[a,b] Xiaozhong Qu,*[a,b] Feiyan Zhu,[a] Yongri Liang,[b] Fuxin Liang,[b] Qian Wang,[b] Jiaoli Li,[b] Zhibo Li[b] and Zhenzhong Yang*[b]

Received (in XXX, XXX) Xth XXXXXXXXX 20XX, Accepted Xth XXXXXXXXX 20XX
DOI: 10.1039/b000000x

Complex formation between polymers and organic molecules is an interesting topic in polymer physics. Compared to the influence of small molecules on polymer assembly, there are fewer examples demonstrating the effect of polymer on the supramolecular structures formed by organic molecules. In this paper, we first prove that doxorubicin (DOX), a common anti-tumour drug, assembles fibril-like aggregates in phosphate buffer (pH 7.4), and then show that the assembly of DOX was influenced by the complexation with an amphiphilic poly (amino acid) derivative, i.e. cholate grafted poly-L-lysine (PLL-CA). With the PLL-CA, the DOX fibrils converted to helix structured nano-spindles, whilst the presence of PLL led to minor change on the morphology of PLL/DOX complex compared to the DOX aggregates, which is attributed to the amplitude of intermolecular interactions. As a DNA intercalating agent, the aggregation of DOX on its biofunctionality was also investigated, showing that the formation of fibril assemblies was unfavourable for cellular internalization of DOX, and caused lower cytotoxicity to DOX resistance MCF-7 cells, whereas the polymer/DOX complexes gained an improved cell uptake on the MCF-7/ADR cell line due to an enhanced electrostatic interaction between the complexes and the cell membrane.

Introduction

While the influence of small molecules on polymer assembly has been extensively studied, less attention was paid on the effect of polymer complexation on the supramolecular structure of small molecules.[1-3] Nevertheless, the importance on investigating the aggregation behaviour of organic molecules has been recognized. For instance, it is known that the bioactivity of drugs can be altered with their aggregate structure. As an example, nanocrystals of drugs show an improved bioavailability in vivo, due to the diversion of transintestinal pathway and cell internalization property.[4-7] Considering that the therapeutic effect of many drugs is achieved through the incorporation with targeting biomolecules, such as protein and DNA etc,[8-10] fundamental studies on the aggregation of drug molecules with macromolecules provide a bottom-up understanding of the drug performances and may benefit the future drug design and other pharmaceutical or biotechnological applications of the drugs.[11-13]

In chemistry field, the aggregation of small molecules are basically affected by environmental conditions such as ion strength, pH and temperature etc,[14,15] and are also influenced by the presence of polymer. For example, Huang et. al. found that the inclusion of poly(ethylene glycol)-block-branched polyethyleneimine varied the crystallization state of the potassium salt of 3,4,9,10-perylenetetracarboxylic acid and gains microbelt-like composites.[16] Yu et. al. showed that an anionic dye led a peptide amphiphile C_{12}-Aβ(11-17) to form nanofibrils which exhibits an aggregation-induced pH sensitive emission feature.[17]

Doxorubicin (DOX) is one of the most widely used anticancer drug, despite it has the major limitation of high cytotoxicity[18] and meanwhile the therapeutical efficiency could be impeded by multidrug resistance (MDR).[19-21] Drug delivery systems based on nano- and micro-spheres have been studied for decades in order to overcome the barriers for the transportation of drugs into cells, such as by changing their internalization pathway, in order to avoid the drug efflux mediated by P-gp which happens on the diffusion pathway of free drugs.[22] Liposome has been used as a carrier of DOX.[23] In some of those studies, it is noted that DOX forms bundle-shaped aggregates consisted of nanofibers in the cavity filled with citrate or sulfate ions at acidic to neutral pH (i.e. 4-7).[24-27] And the aggregation of DOX prevented the drug molecules from invagination into the membrane edge of the liposomes, which is thought to happen for free DOX molecules.[24] These results imply that the non-spheral aggregates of DOX may not be favourable for penetrating bilayers like cell membrane. Since DOX acts as a DNA intercalating agent to inhibit further DNA and RNA biosynthesis, which performs inside the cancer cells,[28] it is of interest to further investigate possible aggregation of DOX under physiological condition and to clarify the influences of the aggregation, once occurred, on cell penetration and the cytotoxicity of the drug.[29]

In this paper, we prove that DOX indeed forms fibril-like

assemblies in phosphate buffer (PB, 10 mM pH 7.4), and the formation of DOX fibrils decreases the drug's intercellular transportation efficiency to DOX resistance MCF-7 (MCF-7/ADR) cells and thus reduces the ability to cause cell apoptosis. Furthermore, by complexation with a cationic poly (amino acid) and its amphiphilic derivative, i.e. poly-L-lysine (PLL) and cholate grafted PLL (PLL-CA) (chemical structures see Figure 1), we investigated the role of weak interactions on the aggregation behaviour of DOX as well as on the formation of supramolecular structure formed by the polymers and the drug.

Experimental Section

Materials

Poly-L-lysine hydrobromide (M_W =15-30 kDa) and fluorescein isothiocyanate (FITC) were purchased from Sigma-Aldrich (St. Louis, US). Doxorubicin hydrochloride (DOX) was supplied by Huafeng Lianbo Technology Co. (Beijing, China). Cholate grafted Poly-L-lysine (PLL-CA) was synthesized via a two step procedure according to previous works.[30,31] The CA substitution level for the PLL-CA used in this work was determined by elemental analysis and ^{1}H NMR to be 25 % to the lysine segments. Solvents and other compounds were obtained from Beijing Chemical Reagents Company, China.

Synthesis of FITC-labeled PLL and PLL-CA

PLL or PLL-CA was dissolved in anhydrous DMSO and FITC isocyanate was added in a ratio of roughly one fluorophore per 50 lysine monomers with vigorous stirring. After reacting for 12 h at 25 °C, the reaction mixture was applied to an open-column filled with Sephadex LH-20 gel (GE Healthcare, Sweden) and eluted using DMSO to separate FITC-Polymer from unreacted FITC.

Preparation of DOX assembly and polymer/DOX co-assemblies

DOX or a mixture of polymer and DOX with varied weight ratio was dissolved in methanol in a 25 mL round bottomed flask. The solution was slowly evaporated with a rotary evaporator under vacuum to form a thin film, and further dried for 3-6 h to ensure a complete removal of residual organic solvent. Subsequently, phosphate buffer (PB, 10 mM, pH 7.4) was added into the flask to get dispersion at a fixed polymer concentration. The dispersion was sonicated in a bath sonicator for 1 h at 30 °C, then stirred for 30 min at room temperature and kept at 4 °C prior to further characterizations.

Transmission electron microscopy

Transmission electron microscopy (TEM) was carried out on a JEM-1011 microscope at an operating voltage of 100 kV. The DOX dispersions as prepared above were dropped onto carbon-coated copper grids, followed by staining using 0.5% phosphotungstic acid solution (pH=7.4), and then air dried.

Cryogenic transmission electron microscopy (cryo-TEM) samples were prepared in a controlled environment vitrification system (CEVS) at a preset temperature. The prepared dispersions were annealed in the CEVS system for 10 min at each temperature prior to sample preparation. Then, 5 μL of sample solution was loaded onto a carbon-supported lacey TEM grid, which was held by tweezers. The excess solution was blotted with a piece of filter paper, resulting in the formation of thin films suspended the mesh holes, and the samples were quickly plunged into a reservoir of liquid ethane (cooled by liquid nitrogen) at its melting temperature. The vitrified samples were then stored in liquid nitrogen until they were transferred to a cryogenic sample holder (Gatan 626) and examined using a JEM 2200FS TEM (200 kV) at about -174 °C. The images were recorded on a Gatan multiscan CCD and processed with Digital Micrograph.

Circular dichroism

Circular dichroism (CD) spectra were recorded on a JASCO J-815 spectrophotometer at room temperature using 0.1 mm quartz cells. Scans were obtained in a range between 190 and 700 nm by taking points at 0.5 nm, with an integration time of 0.5 s. Five spectra were averaged to improve the signal-to-noise ratio.

X-ray diffraction and scattering measurements

Powder X-ray diffraction (XRD) was measured on a Rigaku D/max-2500 X-ray diffractometer with Cu Kα radiation (λ=0.154 nm) as the X-ray source. Wide-angle X-ray scattering (WAXS) measurements were performed at BL14B1 beamline in Shanghai Synchrotron Radiation Facility (SSRF), China. Two-dimensional (2D) Mar345 detectors were used to collect the 2D WAXS patterns. The wavelength of the incident X-ray was 1.24 Å, and the sample to detector distance (SDD) was 224.5 mm. Silicon powder was used as standard material for calibration of the scattering vector of WAXS.

UV-Vis spectrophotometry

The absorption and transmittance spectra of dispersions were collected in the range of 400-700 nm on a TU-1901 UV-Vis spectrophotometer. The fluorescence spectra of DOX or PLL/DOX dispersions with a series of concentrations were recorded using a fluorescence spectrophotometer (Cary Eclipse, Varian) with an excitation wave-length of 485 nm. The width of the excitation and emission slits is 5 nm.

^{1}H NMR measurements

^{1}H NMR was recorded on a Bruker AVIII 500 WB spectrometer at 298 K. The NMR samples were prepared via the thin film rehydration method as mentioned above at a fixed DOX concentration of 300 μg/mL, expect the films of specific samples were hydrated using 10 mM PB with D_2O/H_2O (1:9 v/v) as solvent. WATERGATE (water suppression by gradient-tailored excitation) and jump-and-return techniques were used to suppress the water peak. Chemical shifts were referenced to micro-amount of the residual methanol at 3.27 ppm.

Cell uptake

MCF-7/ADR cells (European Collection of Cell Cultures, UK) were cultured using Roswell Park Memorial Institute 1640 media (RPMI-1640, Gibco) supplemented with 10% fetal bovine serum (FBS, Gibco), 1% $_L$-glutamine, antibiotics penicillin (100 IU/mL), and streptomycin (100 IU/mL) and plated on microscope slides in a culture dish at 5×10^4 cells/well. After 24 h, the culture medium was replaced with the medium dispersion of DOX, PLL/DOX and PLL-CA/DOX aggregates. After incubation at 37 °C and 5% CO_2 for 30 min, the medium was removed, and the cells on

microscope plates were washed three times with ice-cold PBS. The cells were then fixed with 4% formaldehyde for 20 min and further washed with PBS, and then stored at 4 °C. Fluorescence images of cells were observed using a FV 1000-IX81 confocal laser scanning microscope (CLSM, Olympus, Japan) with an excitation wavelength of 488 nm and emission wavelength of 500-550 nm for FITC and 560-660 nm for DOX.

Cytotoxicity

The cytotoxicity of DOX solution and the dispersion of DOX aggregates was evaluated on MCF-7/ADR cell line by CCK assays on Cell Counting Kit-8 (Dojindo Laboratories). Sample dispersion containing DOX aggregates was prepared by rehydrating the DOX thin film using culture media containing 10 mM phosphate buffer. And as a control sample, free drug solution was also prepared via diluting concentrated water solution of DOX (500 μg/mL) to desired concentration using medium. The control sample was checked using TEM and viewed few fibril-like aggregates during a period of 8h, which was the longest time for the test. MCF-7/ADR cells were seeded in 96-well plates at a density of 2×10^4 cells/well for 1 d. Then DOX samples with different concentrations were added and the cells were cultured for a given time at 37 °C. After that, the culture medium was replaced with CCK-8 reagent solution and cells were further incubated for 3 h at 37 °C. The absorbance at 450 nm of each well was measured using a microplate reader. The cell viability (%) was determined by comparing the absorbance with control wells containing cell without DOX.

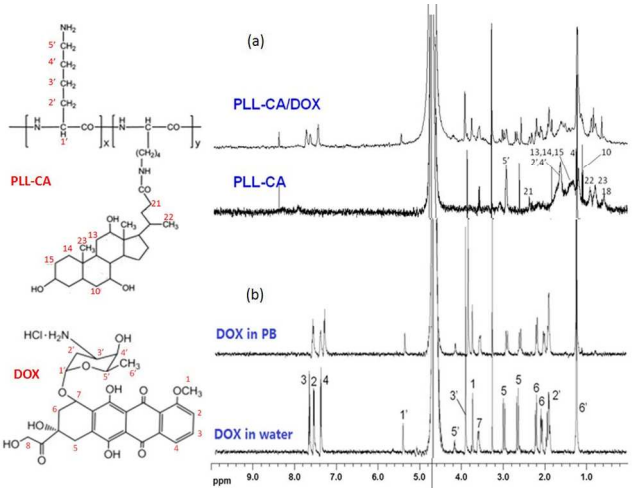

Figure 1. Chemical structure of PLL-CA (up left) and DOX (down left). ^{1}H NMR spectra, (a) PLL-CA and PLL-CA/DOX complex in deuterated PB (10 mM in 1:9 v/v of D2O/H2O), (b) DOX in deuterated water and deuterated PB (b). The weight ratio of polymer/DOX and the concentration of DOX were 1:0.5 and 300 μg/mL respectively.

Results and Discussion

Aggregation behaviour of Doxorubicin

Fibril-like aggregates of DOX were observed by cryo-TEM in PB solution (10 mM, pH 7.4) at DOX concentrations above 80 μg/mL (~0.14 mM) (Figure 2). Similar structure was seen in TEM image (Figure 2), with some thicker helix shaped aggregates being also observed, probably owing to a secondary assembly of the DOX fibrils during the concentration of solute in the TEM sample preparation procedure. Previous reports described that DOX forms aggregates in the cavity of liposomes containing acidic citrate or sulfate buffer, but at much higher drug concentrations (0.5-1.5 mM) and displaying a very different morphology, i.e. bundle-shaped aggregates.[25] Besides, it is worth noticing that the fibril-like aggregates could be gained using ultrasonication method on the PB dispersion of DOX powder, and the DOX aggregates dissociated with dilution. These indicate that the assembly of DOX molecules is thermodynamic driven. The aggregation of DOX was attributed to the bridge effect of multianion.[25-27] In our case, we also expect that the phosphate anion plays as the same role as to join the neighbour DOX molecules, since no aggregate was found in case the DOX was rehydrated by water. XRD on freeze-dried PB solution of DOX shows that the crystallizaiton of both DOX and phosphate is significantly restricted (Figure S1), and therefore confirms the interaction between the salt and the drug molecules. Li et al. suggested a twisting hexagonal lattice model of DOX aggregates generated from the stacking of drug molecules in citrate buffer based on TEM images and XRD patterns got from centrifugated samples.[25] Herein, WAXS on DOX in PB dispersion (300 μg/mL, 0.5 mM) reveals only a broad peak centred at 22.2° (Figure 3a). CD was then used to characterize the conformation of DOX molecules in solution since the previous work observed an obvious change on CD spectrum of DOX around 300-600 nm due to the formation of aggregates in citrate solution (pH~4).[25] However, our CD results exhibit no conformation change of DOX molecules in PB when compared to that in water (Figure 3b). The above results show that DOX assembles into a novel microstructure in an environment close to body condition, i.e. phosphate-buffered system, giving a linear morphology while the molecules are not significantly ordered.

In addition to counterion mediated electrostatic interaction, other weak interactions are also factors that determine the aggregation structure of organic molecules. In our case, ^{1}H NMR demonstrates that the linewidth of the resonance of DOX protons in the anthracycline ring (2-CH, 3-CH and 4-CH, 7.2-7.8 ppm) and the amino sugar (1'-CH, 5'-CH, 6'-CH_3, 5.4, 4.2 and 0.8 ppm) becomes larger in PB solution (10 mM in D_2O/H_2O 1:9 v/v) than in D_2O/H_2O (1:9 v/v), indicating that these corresponding protons are under a more confined condition when in PB (Figure 1). Thus, it is likely that in addition to the electrostatic coupling, the anthracycline rings and the amino sugars in the DOX molecules interact via van de Waals forces and hydrogen bonding respectively, which restrict the mobility and hence decrease the diffusion rate of the drug molecules,[32] leading to a phase separation of DOX due to the dynamic asymmetry of the dispersion.[33] Considering that DOX is a kind of rigid molecule, the multiple interactions respectively in the hydrophobic and polar regions of the molecule will cause a parallel orientation of DOX and thus gain a fibril structured aggregate.

To further investigating the rationale of the DOX aggregation, a polycation, i.e. PLL, was introduced. With a pKa of ~9.4 and ~8.25 for PLL[34] and DOX[12] respectively, there would be no direct electrostatic interaction between the polymer and the drug at acidic and neutral pHs. However it is shown that the addition of PLL led to the formation of polymer/DOX co-assemblies at pH

7.4 in PB buffer, as proven by the overlapping of FITC-labelled PLL fluorescence and DOX fluorescence in the CLSM images (Figure 2). Nevertheless, the PLL/DOX complex keeps a similar morphology as that of the DOX aggregate despite the change of polymer/drug ratio (Figure 2), although the stability of dispersion is significantly enhanced (Figure 3c). It was also found that the PLL/DOX aggregates also existed at acidic PB buffer, e.g. pH 5.0, but dissociated at a basic pH around 10, a value above the pKa of DOX and PLL (Figure S2). The results prove the bridging effect of phosphate anions between the positively charged amino groups in DOX and the lysine segments, and furthermore imply that the PLL chains are majorly distributed surrounding on the surface of PLL/DOX fibrils. Meanwhile, since the complexation of PLL does not disrupt the aggregation structure formed by the DOX molecules, it can infer that electrostatic force is not the only interaction that induces the formation of DOX fibrils.

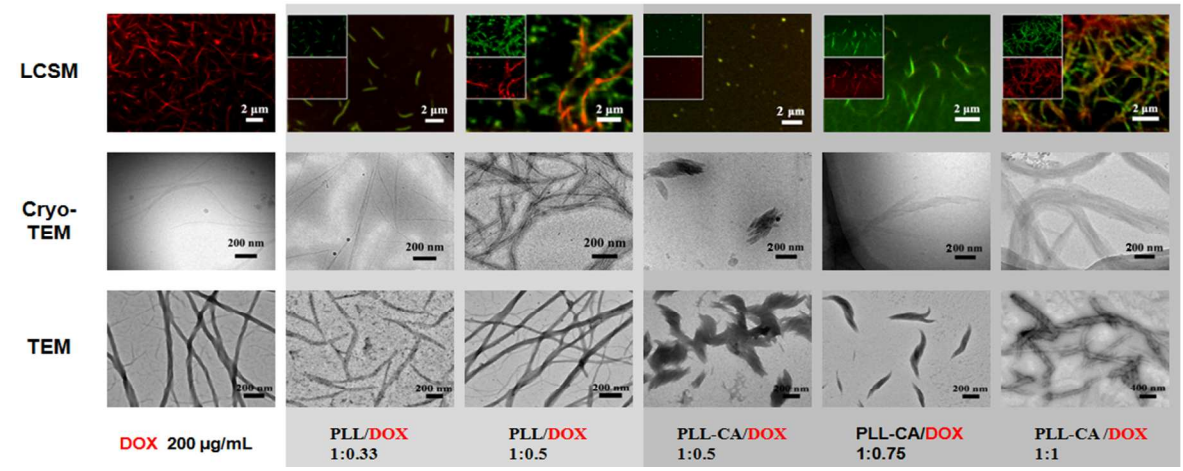

Figure 2. Merged CLSM (top line), cryo-TEM (middle line) and negatively stained TEM (bottom line) images of DOX, PLL/DOX complex and PLL-CA/DOX complex at different polymer/DOX weight ratio in PB buffer (pH =7.4). Inset images of CLSM, up: FITC channel, down: DOX channel. PLL and PLL-CA were labeled with FITC. The polymer concentration was fixed at 500 μg/mL.

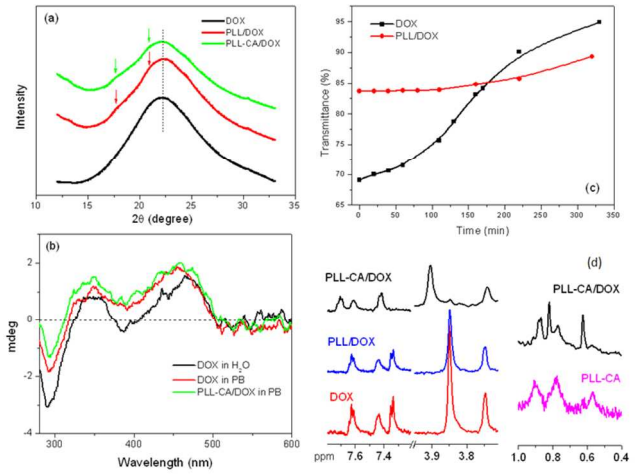

Figure 3. (a) WAXS of DOX, PLL/DOX and PLL-CA/DOX in PB buffer at pH 7.4. (b) CD spectra of DOX and PLL-CA/DOX complex in water or PB buffer. (c) The stability of DOX and PLL/DOX dispersions in 10 mM PB buffer at pH 7.4, monitored using UV-vis transmittance at 600 nm. The increase of transmittance indicates the precipitation of DOX aggregates. (d) Enlarged ^{1}H NMR spectra of PLL-CA, DOX, PLL/DOX, and PLL-CA/DOX in deuterated PB (D_2O/H_2O, 1:9 v/v) at 25 ^oC. The ratio of poymer/DOX was fixed at 1:0.5 w/w. The concentration of DOX was 100 μg/mL for CD analysis while 300 μg/mL was used in WAXS, UV-vis and ^{1}H NMR tests.

Amphiphilic cholate grafted PLL was then used as a component to form complex with DOX. As normal drug solubilised micellar systems,[35] PLL-CA could form spherial shaped micelles in aqueous solution due to the amphiphilic nature with DOX solubilised in the hydrophobic microdomain when the drug concentration was below the value for aggregation (e.g. <80 μg/mL). However with DOX concentration of 165-375 μg/mL (PLL-CA/DOX weight ratio was 1:0.33-1:0.75), cryo-TEM and TEM observe hierarchical spindle-like PLL-CA/DOX aggregates consisted of needle-like nanoparticles, while LCSM confirms the complexation of PLL-CA and DOX (Figure 2). The phenomenon is suggested due to the assembly tendency of the drug molecule, but meanwhile the aggregate formation was affected by the hydrophobic moieties of the polymer, i.e. the CA pendants. ^{1}H NMR spectra in Figure 3d demonstrate that with PLL-CA, the chemical shifts of the DOX protons in the anthracycline ring (2-CH, 3-CH and 4-CH, 7.2-7.8 ppm) and the amino sugar (3'-CH and 5'-CH, 3.7-3.9 ppm) move to down field when compared to that in DOX and PLL/DOX dispersions. Meanwhile, the linewidth of the protons in CA group at 0.8-1 ppm becomes narrower in PLL-CA/DOX than that in the neat polymer dispersion (Figure 3d). These results describe that the inclusion of CA results in stronger interaction between DOX and the polymer via the hydrophobic and the H-bond forming groups. Nevertheless, WAXS characterization reveals that the aggregates are still in amorphous state (Figure 3a). Two additional peaks at 17.5 and 20.9^o are assigned to the polymer since they also appear in the curve of the PLL/DOX sample. Besides, fluorescence test shows that self-quench of DOX emission occurs at higher concentration in the presence of PLL-CA, indicating that the polymer has blocked the stacking of the drug molecules (Figure S3). Thus, the role of the CA groups is determined as to insert into the paralleled DOX molecules and prevent the packing to a longer train. This should be the reason that causes the formation of the short needle-like nanoparticle, that is the building block to form the spindle-shaped aggregates. The hypothesis could be supported by the fact that increasing the DOX content will decrease the oblique angle of the needle-like particles and hence

gained thinner PLL-CA/DOX spindles (Figure2, Table S1). And eventually, at a PLL-CA/DOX weight ratio of 1:1, the fibre-like aggregates are formed (Figure 2). These data further confirm that the packing of DOX molecules is organized from a combination of weak interactions.

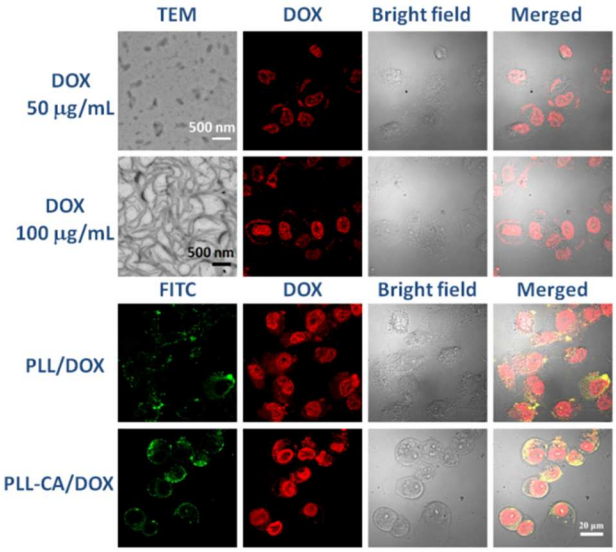

Figure 4. CLSM images of MCF-7/ADR cells treated by DOX dispersion, PLL/DOX and PLL-CA/DOX dispersions for 30 min. The polymers were labelled by FITC. The DOX concentration was 100 μg/mL, and the polymer/drug ratio was 1:1 w/w for both PLL/DOX and PLL-CA/DOX samples. The TEM images show that DOX forms fibril-like aggregates in culture media at a concentration of 100 μg/mL but not at 50 μg/mL.

Internalization of DOX aggregates to tumour cells.

Since it is observed that DOX assembles under physiology condition, the cell binding ability of the DOX aggregates becomes an attractive issue. It was known that DOX can cause drug resistance of tumour cells due to the action of P-gp which pumps out the DOX molecules that have diffused across the membrane.[36-38] In contrast, drug formulations in nanoparticulate form are known being able to transport to the cytoplasm through an endocytosis pathway.[39-42] However, using DOX resistance MCF-7 (MCF-7/ADR) cell line, we found that DOX was still majorly distributed in cell membrane and nuclear regions after 30 min incubation, no matter whether the sample dispersions containing aggregates or not (Figure 4). Such a distribution suggests a diffusion dominating transportation of free drug molecules.[43,44] Comparably, both DOX and polymer fluorescence is seen in the cytoplasm in the PLL/DOX and PLL-CA/DOX treated cells (Figure 4). Although the influence of particle shape on cell uptake is not very clear so far,[45] indeed numbers of reports have shown that non-spheral nanoparticles can internalize into cells through either endocytosis or phagocytosis pathway,[46-48] and the efficiency is related to not only the length-to-diameter ratio, but also the surface properties.[49] According to the results shown here, it suggests that the DOX aggregates are not favourable for its internalization probably due to the lack of interaction with cell membrane, i.e. the amino group in DOX was coupled with salt ions. In contrast, the polymer/DOX complexes, regardless their morphology, i.e. fibril or spindle shaped, displayed an efficient endocytosis, because of the enhancement of electrostatic force between the complexes and the cells by the inclusion of more amino groups from PLL.

The influence of DOX aggregation on its therapeutic efficiency was examined by comparing the cytotoxicity of DOX formulations containing and not containing aggregates on MCF-7/ADR cells. Figure 5 shows that the aggregate containing formulation caused poorer apoptosis of the cells with an IC_{50} of 210 μg/mL after an incubation of 8 h, significantly higher than the formulation prepared from water (IC_{50} = 175 μg/mL) which contains few aggregates within experimental duration. Therefore, this work suggests that the aggregation ability of DOX would be considered in the future design of delivery vehicles, especially for those intending to control the DOX release at the tumour site,[50] since letting DOX release outside cancer cells, even in high level, may lead to less desirable efficiency as expected, because the possible aggregation of DOX molecules will keep the portion of drug to stay extracellularly.

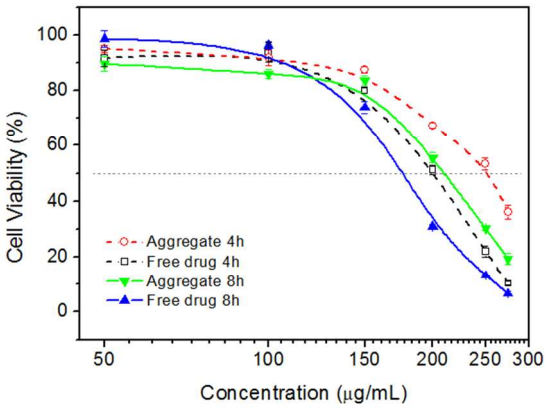

Figure 5. Cytotoxicity of DOX formulations containing or not containing fibril-like aggregates. The cell viability between the two kinds of samples has significant difference at DOX concentration points higher than 150 μg/mL (p<0.05, Student's t-test).

Conclusions

In this work, we demonstrate that doxorubicin assembles into fibril-shaped aggregates under physiological condition (phosphate buffer, pH 7.4) and figure out the influence of physical interactions between DOX and surrounding polymer on the microstructure of the aggregate. It is recognized that a combined effect of weak interactions between DOX molecules causes the formation of one-dimensional morphology of DOX assemblies while are in an amorphous state in molecular level. Polycations and its amphiphilic derivative can form complexes with the drug, changing the surface property and the morphology of the aggregates, depending on the type and strength of the intermolecular interactions. It is also shown that the formed DOX fibrils are not favourable for internalization into tumour cells and thus lead to lower cytotoxicity of the aggregates compared to free drug. As multi-drug resistance is a big challenge for cancer treatment which normally forces high level of DOX dosage but may give limit improvement, we hope future pharmacological works on the DOX aggregates will further clarify the therapeutic rationale of the drug.

Acknowledgements

Dr. Junfeng Xiang of Institute of Chemistry is appreciated for his helps on the ^{1}H NMR tests. The work is supported by Natural Science Foundation of China (21274115, 51233007), and MOST (2012CB933200).

Notes and references

[a] *University of Chinese Academy of Sciences, Beijing 100049, China. Tel: 86 10 69671760; E-mail: quxz@iccas.ac.cn*
[b] *State Key Laboratory of Polymer Physics and Chemistry, Institute of Chemistry, Chinese Academy of Sciences, Beijing 100190, China. Fax: 86 10 62559373; Tel: 86 10 82619206; E-mail: yangzz@iccas.ac.cn*

† Electronic Supplementary Information (ESI) available: Supplementary figures and table. See DOI: 10.1039/b000000x/

1 H. Cui, Z. Chen, S. Zhong, K. L.Wooley and D. J. Pochan, *Science* 2007, **317**, 647.
2 S. Zhong, H. Cui, Z. Chen, K. L.Wooley and D. J. Pochan, *Soft Matter* 2008, **4**, 90.
3 Z. Sun, F. Bai, H. Wu, S. K. Schmitt, D. M. Boye and H. Fan, *J. Am. Chem. Soc.* 2009, **131**, 13594.
4 L. Gao, G. Y. Liu, J. L. Ma, X. Q. Wang, L. Zhou, X. Li and F. Wang, *Pharm. Res.* 2013, **30**, 307.
5 L. Gao, G. Y. Liu, J. L. Ma, X. Q. Wang, L. Zhou and X. Li, *J. Control. Release* 2012, **160**, 418.
6 E. Merisko-Liversidge, G. G. Liversidge and E. R. Cooper, *Eur. J. Pharm. Sci.* 2003, **18**, 113.
7 Y. Tian, L. Bromberg, S. N. Lin, T. A. Hatton and K. C. Tam, *J. Control. Release* 2007, **121**, 137.
8 V. Lhiaubet-Vallet, F. Bosca and M. A. Miranda, *J. Phys. Chem.* B 2007, **111**, 423.
9 N. Li, Y. Ma, C. Yang, L. P. Guo and X. R. Yang, *Biophys. Chem.* 2005, **116**, 199.
10 Y. Porat, Y. Mazor, S. Efrat and E. Gazit, *Biochemistry* 2004, **43**, 14454.
11 K. A. Janes, M. P. Fresneau, A. Marazuela, A. Fabra and M. J. Alonso, *J. Control. Release* 2001, **73**, 255.
12 M. V. Kitaeva, N. S. Melik-Nubarov, F. M. Menger and A. A. Yaroslavov, *Langmuir* 2004, **20**, 6575.
13 Y. Tian, L. Bromberg S. N. Lin, T. A. Hatton and K. C. Tam, *J. Control. Release* 2007, **121**, 137.
14 G. M. Whitesides, J. P. Mathias and C. T. Seto, *Science* 1991, **254**, 1312.
15 H. Z. Wang, C. Qian and M. Roman, *Biomacromolecules* 2011, **12**, 3708.
16 M. Huang, U. Schilde, M. Kumke, M. Antonietti and H. Colfen, *J. Am. Chem. Soc.* 2010, **132**, 3700.
17 D. F. Yu, M. L. Deng, C. Q. He, Y. X. Fan and Y. L. Wang, *Soft Matter* 2011, **7**, 10773.
18 F. Arcamone, *Cancer Res.* 1985, **45**, 5995.
19 P. D. W. Eckford and F. J. Sharom, *Chem. Rev.* 2009, **109**, 2989.
20 M. Kavallaris, *Nat. Rev. Cancer* 2010, **10**, 194.
21 P. Savage, J. Stebbing, M. Bower and T. Crook, *Nat. Clin. Pract. Oncol.* 2009, **6**, 43.
22 Z. Ge and S. Liu, *Chem. Soc. Rev.* 2013, **42**, 7289.
23 M. B. Bally, R. Nayar, D. Masin, M. J. Hope, P. R. Cullis and L. D. Mayer, *Biochim. Biophys. Acta.* 1990, **1023**, 133.
24 P. R. Harrigan, K. F. Wong, T. E. Redelmeier, J. J .Wheeler and P. R. Cullis, *Biochim. Biophys. Acta.* 1993, **1149**, 329.
25 X. G. Li, D. J. Hirsh, D. Cabral-Lilly, A. Zirkel, S. M. Gruner, A. S. Janoff and W. R. Perkins, *Biochim. Biophys. Acta.* 1998, **1415**, 23.
26 D. D. Lasic, B. Ceh, M. E. A. Stuart, L. Guo, P. M. Frederik and Y. Barenholz, *Biochim. Biophys. Acta.* 1995, **1239**, 145.
27 S. A. Abraham, K. Edwards, G. Karlsson, S. MacIntosh, L. D. Mayer, C. McKenzie and M. B. Bally, *Biochim. Biophys. Acta.* 2002, **1565**, 41.
28 G. Minotti, P. Menna, E. Salvatorelli, G. Cairo and L. Gianni, *Pharmacol. Rev.* 2004, **56**, 185.
29 L. Gallois, M. Fiallo and A. Garnier-Suillerot, *Biochim. Biophys. Acta.* 1998, **1370**, 31.
30 J. Gu, W. P. Cheng, C. Hoskins, P. K. T. Lin, L. Zhao, L. Zhu, X. Qu and Z. Yang, *J. Microencapsul.* 2011, **28**, 752.
31 L. Zhu, L. Zhao, X. Qu and Z. Yang, *Langmuir* 2012, **28**, 11988.
32 H. Tanaka, *J. Phys.: Condens. Matter* 2000, **12**, R207.
33 H. Tanaka, *Adv. Mater.* 2009, **21**, 1872.
34 S. Fukushima, K. Miyata, N. Nishiyama, N. Kanayama, Y. Yamasaki and K. Kataoka, *J. Am. Chem. Soc.* 2005, **127**, 2810.
35 E. S. Lee, Z. Gao, D. Kim, K. Park, I. C. Kwon and Y. H. Bae, *J. Control. Release* 2008, **129**, 228.
36 N. M. Maraldi, N. Zini, S. Santi, K. Scotlandi, M. Serra and N. Baldini, *Biol. Cell.* 1999, **91**, 17.
37 A. Rajagopal and S. M. Simon, *Mol. Biol. Cell.* 2003, **14**, 3389.
38 Y. C. Wang, F. Wang, T. M. Sun and J. Wang, *Bioconjugate Chem.* 2011, **22**, 1939.
39 M. Han, Q. Lv, X. Tang, Y. Hu, D. Xu, F. Li, W. Liang and J. Gao, *J. Control. Release* 2012, **163**, 136.
40 Y. Wang, F. Wang, T. Sun and J. Wang, *Bioconjugate Chem.* 2011, **22**, 1939.
41 K. Na, E. S. Lee and Y. H. Bae, *J. Control. Release* 2003, **91**, 103.
42 Z. Gao, L. Zhang and Y. Sun, *J. Control. Release* 2012, **162**, 45.
43 X. Xiong, A. Mahmud, H. Uluda and A. Lavasanifar, *Pharm. Res.* 2008, **25**, 2555.
44 C. Peetla, R. Bhave, S. Vijayaraghavalu, A. Stine, E. Kooijman and V. Labhasetwar, *Mol. Pharm.* 2010, **7**, 2334.
45 J. A. Champion, Y. K. Katare and S. Mitragotri, *J. Control. Release* 2007, **121**, 3.
46 J. A. Champion and S. Mitragotri, *Proc. Natl. Acad. Sci.* 2006, **103**, 4930.
47 W. Wang, S. Li, L. Mair, S. Ahmed, T. J. Huang and T. E. Mallouk, *Angew. Chem. Int. Ed.* 2014, **53**, 3201.
48 J. B. Gilbert, J. S. O'Brien, H. S. Suresh, R. E. Cohen and M. F. Rubner, *Adv. Mater.* 2013, **25**, 5948.
49 S. Mmitragotri1 and J. Llahann, *Nat. Mater.* 2009, **8**, 15.
50 C. Ding, J. Gu, X. Qu and Z. Yang, *Bioconjugate Chem.* 2009, **20**, 1163.

Graphical Abstract

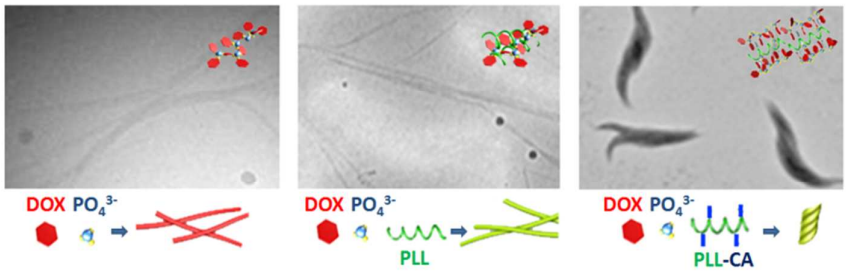

Doxorubicin forms fibril-like aggregates in phosphate buffer, and complexes with poly-L-lysine and cholate grafted poly-L-lysine.